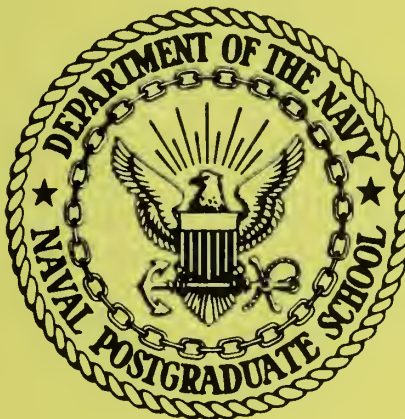NPS-57Bp74071

NAVAL POSTGRADUATE SCHOOL
Monterey, California

AIRCRAFT FUEL TANK VULNERABILITY TO HYDRAULIC RAM:

MODIFICATION OF THE NORTHROP FINITE ELEMENT
COMPUTER CODE BR-1 TO INCLUDE FLUID-STRUCTURE INTER-
ACTION--THEORY AND USER'S MANUAL FOR BR-1HR

by

R. E. BALL

JULY 1974

Final Report for Period 1 July 1973-30 June 1974

Approved for public release; distribution unlimited.

Prepared for:
Air Force Flight Dynamics Laboratory
Wright-Patterson AFB, OH 45433

NAVAL POSTGRADUATE SCHOOL

Monterey, California

Rear Admiral I. W. Linder, USN   Jack Borsting

Superintendent   Provost

This report was prepared by:

REPORT DOCUMENTATION PAGE		READ INSTRUCTIONS BEFORE COMPLETING FORM
1. REPORT NUMBER NPS-57Bp74071	2. GOVT ACCESSION NO.	3. RECIPIENT'S CATALOG NUMBER
4. TITLE *(and Subtitle)* AIRCRAFT FUEL TANK VULNERABILITY TO HYDRAULIC RAM: MODIFICATION OF THE NORTHROP FINITE ELEMENT COMPUTER CODE BR-1 TO INCLUDE FLUID-STRUCTURE INTERACTION--THEORY AND USER's MANUAL FOR BR-1HR		5. TYPE OF REPORT & PERIOD COVERED Final Report 1 July 1973 - 30 June 1974
		6. PERFORMING ORG. REPORT NUMBER
7. AUTHOR(*s*) R. E. BALL		8. CONTRACT OR GRANT NUMBER(*s*)
9. PERFORMING ORGANIZATION NAME AND ADDRESS NAVAL POSTGRADUATE SCHOOL MONTEREY, CA 93940		10. PROGRAM ELEMENT, PROJECT, TASK AREA & WORK UNIT NUMBERS FY 1456-74-00001
11. CONTROLLING OFFICE NAME AND ADDRESS AIR FORCE FLIGHT DYNAMICS LABORATORY WRIGHT-PATTERSON AFB, OH 45433		12. REPORT DATE July 1974
		13. NUMBER OF PAGES 35
14. MONITORING AGENCY NAME & ADDRESS *(If different from Controlling Office)*		15. SECURITY CLASS. *(of this report)* UNCLASSIFIED
		15*a.* DECLASSIFICATION/DOWNGRADING SCHEDULE

16. DISTRIBUTION STATEMENT *(of this Report)*

Approved for public release; distribution unlimited.

17. DISTRIBUTION STATEMENT *(of the abstract entered in Block 20, if different from Report)*

Aircraft Survivability
Aircraft Vulnerability
Fuel Cells
Hydraulic Ram

18. SUPPLEMENTARY NOTES

19. KEY WORDS *(Continue on reverse side if necessary and identify by block number)*

20. ABSTRACT *(Continue on reverse side if necessary and identify by block number)*
The finite element digital computer code BR-1, developed by the Northrop Corporation, for predicting the effects of internal air blast on combat aircraft structures is modified to include the effects of compressible fluid-structure interaction. The true interaction phenomenon is approximated by the piston theory. The modification enables the code to be used to predict the structural response of aircraft fuel tanks subjected to penetrating bullets and fragments. It can also be used in many other

DD _{1 JAN 73} FORM 1473 EDITION OF 1 NOV 65 IS OBSOLETE
(Page 1) S/N 0102-014-6601 |

fluid-structure interaction problems. This report contains the theory, the modifications, and the additional instructions required to operate the modified code, called BR-1HR. The code is operational on the IBM 360/67 in FORTRAN IV, Level H.

DD Form 1473 (BACK)
1 Jan 73
S/N 0102-014-6601

Unclassified
SECURITY CLASSIFICATION OF THIS PAGE(When Data Entered)

iii

TABLE OF CONTENTS

I. INTRODUCTION

A. Background

The Northrop Corporation, under Air Force funding, has developed a finite element digital computer code, called BR-1, for predicting the inelastic, large deflection, transient response of combat aircraft skin-rib-stringer structures when subjected to internal air blast loading. The finite elements considered are flat rectangular plates and beam stiffeners. The theory, user's manual and code listing are given in References 1 and 2. The Air Force Flight Dynamics Laboratory wanted the BR-1 code modified so that it could be used to predict the response of aircraft fuel tank walls when subjected to fluid pressures due to projectiles passing through the fuel in the tank. The intense pressure and momentum in the fuel due to the penetrating projectile is referred to as the hydraulic ram loading. This report describes the modifications to the IBM version of the BR-1 code to account for the fluid (fuel) - structure (tank wall) interaction that occurs when bullets and metal fragments penetrate into aircraft fuel tanks. The modified code is called BR-1HR. The interaction between the compressible fluid and the structure is approximated by the piston theory. The code can also be used for many other compressible fluid-structure interaction problems.

B. Piston Theory

The total nonlinear problem of the response of a tank containing a fluid and subjected to a high speed penetrating projectile is extremely complex and presently defies analytical treatment. In general, the

2

equations for the fluid stresses and motion are coupled to those for the wall stresses and motion due to the continuity at the fluid-structure interface (3). One procedure for approximating the fluid-structure interaction phenomenon is the piston theory (4). This theory has been in use since the early 1940's when it was applied to the study of the effect of underwater explosions on ship plates. It provides the correct solution to the one-dimensional propagation of stresses in an acoustic medium due to a moving boundary. Several recent studies have been made to determine its accuracy when applied to two dimensional fluid-structure interaction problems (4,5).

Application of the piston theory to the interaction problem allows the structure equations and fluid equations to be uncoupled. The response of the wall is computed using the conventional structural response equations, with the normal pressure on the wall p given by

$$p = p_o + \rho c\,(v_i - \dot{w}) \tag{1}$$

where p_o and v_i are the incident pressure and velocity of the fluid at the wall respectively, ρ is the fluid density, c is the acoustic velocity in the fluid, and $\dot{w}$ is the wall velocity*. The pressure, p_o, and velocity, v_i, are the pressure and velocity that would exist in the fluid if the interface was not there, i.e., p_o and v_i do not contain any "local" reflected effects. However, effects on p_o and v_i due to earlier reflections from other walls and free surfaces should be considered. In other words, p_o and v_i are the loading components due to

---

*A dot above a variable denotes a derivative with respect to time.

the free field and the scattered effects. The loading component due to the wall velocity $\dot{w}$ is called the radiation pressure.

C. The NWC Hydraulic Ram Computer Code

In order to use the piston theory to compute the tank wall response, it is necessary to know the incident fluid pressure p_o and velocity v_i over the entire fluid-wall interface as a function of time. In conjunction with this project Lundstrom, at the Naval Weapons Center, has developed a digital computer code that predicts the fluid pressures and velocities p_o and v_i throughout a rectangular body of fluid due to a penetrating ballistic projectile. The model is based upon replacing the projectile by a line of sources whose strength is determined by an energy balance between the kinetic and potential energy of the fluid and the energy loss due to drag forces on the projectile. Reflections from the structure-fluid interface are accounted for by considering the fluid boundary to be either stress free or rigid*. An extensive series of tests were performed at the Naval Weapons Center to obtain detailed pressure measurements for a variety of projectiles under a wide range of impact conditions. This data allowed the selection of important parameters such as tumbling distance, jacket stripping, etc., to be entered into the code. A description of the code and the instructions for operation are given in Reference 7. This code provides the values for p_o and v_i at user specified locations over the structure-fluid interface for the time span of interest.

_____

* A study of the one-dimensional reflection of step pressure waves from typical aircraft fuel tank walls indicates that the stress free surface provides the more accurate approximation (6)

II. MODIFICATION OF THE BR-1 CODE

A. Incorporation of the Piston Theory

The BR-1 code has an option for the user to input a time varying pressure on each panel element. In the piston theory this pressure is the $p_o + \rho c v_i$ of Eq. 1. The other contributor to the wall loading given by Eq. 1 is $\dot{w}$, the wall velocity. Since the BR-1 code does not include damping effects, it is necessary to add the damping term $\rho c \dot{w}$ to the equations of motion.

The BR-1 code solves the set of equations (Eqs. 1 and 2, Ref. 1)

$$[M] \{\ddot{q}*\} = \{F\} - \{P\} - [H] \{q*\} = \{C\} \tag{2}$$

for the vector of global nodal generalized displacements $\{q*\}$ as a function of time. These generalized displacements define the motion of the walls. The vector $\{F\}$ consists of global generalized external and body forces at the nodes of the elements. The matrix $[M]$ is the mass matrix.

The wall pressure p given by Eq. 1 causes external forces at the nodes. The external generalized forces at the nodes of each element in the local coordinate system, $\{f\}$, is given by (Eq. A-47, Ref. 1)

$$\{f\} = \iint_{(Aout)} \left[N_B \right]^T \left\{ T_o \right\} dA \tag{3}$$

where $\left[N_B \right]^T$ is the transpose of the matrix of shape functions $[N]$, evaluated at the surface of the element, Aout is the surface of the element, and $\{T_o\}$ is the vector of applied surface tractions and moments. The order of $\{T_o\}$ is a 5x1 vector. Due to the fluid pressure loading

$$\begin{Bmatrix} T_1 \\ T_2 \\ T_3 \end{Bmatrix} = \begin{Bmatrix} 0 \\ 0 \\ p \end{Bmatrix} \tag{4}$$

where the subscripts denote the coordinates, (T_3 is normal to the element), and p is given by Eq. 1. The fourth and fifth elements of $\{T_o\}$ correspond to applied moments per unit middle surface area of the element, and are zero here. The numerical intergration of Eq. 3 can be accomplished by Gaussian quadrature. However, the $\{f\}$ is obtained in the BR-1 code in a more approximate way by using a lumping approach at the nodes of the element, as is done for the mass matrix evaluation, in order to save computation time. Thus, according to Eq. B-92 of Ref. 1, the external force vector at the rth node of the nth element is given by

$$\{f_{nr}\} = \frac{(x_2-x_1)\ (y_2-y_1)n}{4}\ \frac{p_n}{D_{nr}} \begin{Bmatrix} \theta_2 \\ -\theta_1 \\ 1 \\ 0 \\ 0 \end{Bmatrix}_{nr} \tag{5}$$

where p_n is the magnitude of the pressure on the element*, and $D_{nr} = \sqrt{(1+\theta_1^2+\theta_2^2)}_{nr}$ where θ_1 and θ_2 are the fourth and fifth local generalized displacements at the rth node. They appear here because the pressure is defined in BR-1 as the pressure normal to the deformed surface. The quantities (x_2-x_1) and (y_1-y_2) are the dimensions of the rectangular element.

The pressure p_n in the piston theory is given by Eq. 1, i.e.

$$p_n = p_{on} + (\rho c)_n\ v_{in} - (\rho c)_n\ \dot{w}_{nr} \tag{6}$$

---

* The assumption is made in the programming of BR-1 that the pressure is uniform over each element. This is contrary to the theoretical presentation where the pressure is defined at each node point.

where

$$(\rho c)_n = \begin{cases} \rho c & \text{if the nth element is in contact with the fluid} \\ 0 & \text{if the nth element is not in contact with the fluid.} \end{cases}$$

The variables p_{on} and v_{in} can be determined from the NWC computer code for each element for the time span of interest prior to the computation of the wall response. This data is then input as the known external pressure. The variable $\dot{w}_{nr}$ is an unknown dependent variable and is part of $\{\dot{q}*\}$. Hence, it must be incorporated into the equations of motion, Eq. 2.

The $\{f_{nr}\}$ due to $\dot{w}_{nr}$ is given by

$$\{f_{nr}\} = \frac{-\left(x_2 - x_1\right)\left(y_2 - y_1\right)_n}{4} \quad \frac{(\rho c)_n \, \dot{w}_{nr}}{D_{nr}} \begin{Bmatrix} \theta_2 \\ -\theta_1 \\ 1 \\ 0 \\ 0 \end{Bmatrix}_{nr} \qquad (7a)$$

The global force vector at the rth node, $\{F\}_r$, is related to $\{f_{nr}\}$ in the form

$$\{F\}_r = \sum_{n_r} [J_n]^T \{f_{n\alpha}\}_{\alpha \longleftarrow r} \qquad (7b)$$

where $[J_n]$ is the transformation matrix from the global coordinate system to the nth element local coordinate system, $\sum_{n_r}$ means a summation over all elements containing the node r, and $\alpha \longrightarrow r$ means node α corresponds physically to node r. Since the wall velocity in Eq. 7a is given in terms of the local coordinates, it must be converted to global coordinates. Thus, according to Eqs. A-77 and B-3 of Reference 1,

$$\dot{w}_{nr} = \lfloor J_n^3 \rfloor \{\dot{q}*\}_r \qquad (8)$$

7

where $\lfloor J_n^3 \rfloor$ is the third row of $[J_n]$. Thus, the global external force vector at the rth node $\{F\}_r$ becomes

$$\{F\}_r = \frac{-1}{4} \sum_{n_r} (\rho c)_n [J_n]^T \frac{(x_2 - x_1)(y_2 - y_1)_n}{D_{nr}} [J_n^3] \{\dot{q}^*_r\} \begin{Bmatrix} \dot{\theta}_2 \\ -\dot{\theta}_1 \\ 1 \\ 0 \\ 0 \end{Bmatrix}_{nr} \quad (9)$$

Note that $\{F\}_r$ is nonlinear since $\dot{\theta}_1$ and $\dot{\theta}_2$ are part of $\{\dot{q}^*\}_r$. If the rotations θ_1 and θ_2 are neglected in the computation of $\{F\}_r$, i.e., if the pressure is not truly normal to the deformed surface, $\{F\}$ for the total R nodes of the structure can be given in the form

$$\{F\} = - [D] \{\dot{q}^*\} \quad (10a)$$

where

$$[D] = \begin{bmatrix} [D]_1 & & & \\ & [D]_2 & & 0 \\ & & \ddots & \\ 0 & & & \ddots \\ & & & & [D]_R \end{bmatrix} \quad (10b)$$

and $[D]_r$ is a 6x6 matrix given by

$$[D]_r = \frac{1}{4} \sum_{n_r} (\rho c)_n (x_2 - x_1) (y_2 - y_1)_n [J_n]^T \lfloor J_n^3 \rfloor \quad (10c)$$

8

B. Method of Solution

The BR-1 code solves for $\{q*\}$ at discrete points in time using the explicit finite difference scheme (Eq. A-109, Ref. 1)

$$\{\Delta q*\}_{t_{i+1}} = \{\Delta q*\}_{t_i} + \Delta t \, \{\dot{q}\underset{I}{*}\}_{t_i} + (\Delta t)^2 \, \{\ddot{q}*\}_{t_i} \tag{11}$$

where Δt is the time interval between two time points, i.e.

$$\Delta t = t_{i+1} - t_1$$

and

$$\{\Delta q*\}_{t_{i+1}} = \{q*\}_{t_{i+1}} - \{q*\}_{t_i} \tag{12}$$

The acceleration $\{\ddot{q}*\}_{t_i}$ is obtained from Eq. (2) in the form

$$\{\ddot{q}*\}_{t_i} = [M]^{-1} \, \{C\}_{t_i} \tag{13}$$

The $\{\dot{q}\underset{I}{*}\}$ are due to impulsive loads which are known in the blast loading problem. In the BR-1 code $\{F\}$, $\{P\}$, $\{q*\}$ and $\{\dot{q}\underset{I}{*}\}$ are known at time t_i. Hence, $\{\Delta q*\}_{t_{i+1}}$ and $\{q*\}_{t_{i+1}}$ can be determined using Eqs. 11-13. For our situation, $\{F\}_{t_i}$ contains $\{\dot{q}*\}_{t_i}$, which is unknown. We could approximate $\{\dot{q}*\}_{t_i}$ with the backward finite difference form

$$\{\dot{q}*\}_{t_i} = \{\Delta q*\}_{t_i} / \Delta t \tag{14}$$

If we do, then $\{\dot{q}*\}_{t_i}$ becomes known at t_i, $\{F\}$, and hence $\{C\}$, can be determined at t_i, and the procedure used in BR-1 is directly applicable. On the other hand, if we express $\{\dot{q}*\}_{t_i}$ in the central finite difference form

$$\{\dot{q}*\}_{t_i} = \left(\{\Delta q*\}_{t_{i+1}} - \{\Delta q*\}_{t_i} \right) \Big/ (2\Delta t) \tag{15}$$

then $\{F\}_{t_i}$, and hence $\{C\}_{t_i}$, depends upon $\{\Delta q\}_{t_{i+1}}$. Consequently

$\{\Delta q^*\}_{t_{i+1}}$ appears on both the left and right hand side of Eq. 11. This

requires a new solution procedure. A detailed study of the accuracy

and numerical stability of these two approaches, and a third approach,

when applied to a single degree of freedom, damped oscillator is pre-

sented in the Appendix. The approach where $\{\dot{q}^*\}$ is given by the central

difference expression, Eq. 15, is the one selected based upon the

accuracy and stability properties of this scheme. Its shown in the

Appendix that the maximum value of Δt for a stable solution is $2/\omega$, where

ω is the highest natural undamped frequency. This is identical to the

stability limit on the BR-1 procedure.

Introducing that part of $\{F\}$ due to $\dot{w}$ given by Eq. 10a into Eq. 2
results in the modified equations of motion

$$[M] \{\ddot{q}^*\} + [D] \{\dot{q}^*\} = \{C\} \tag{16}$$

Replacing $\{\ddot{q}^*\}$ with the conventional central difference approximation

$$\{\ddot{q}^*\}_{t_i} = \left(\{q^*\}_{t_{i+1}} - 2 \{q^*\}_{t_i} + \{q^*\}_{t_{i+1}} \right) \Big/ (\Delta t)^2 \tag{17a}$$

is equivalent to obtaining $\{\ddot{q}^*\}_{t_i}$ from Eq. 11 with $\{\dot{q}_I^*\}$ not considered, i.e.

$$\{\ddot{q}^*\}_{t_i} = \left(\{\Delta q^*\}_{t_{i+1}} - \{\Delta q^*\}_{t_i} \right) \Big/ (\Delta t)^2 \tag{17b}$$

according to Eq. 12. Substituting Eq. 15 for $\{\dot{q}^*\}_{t_i}$ and Eq. 17b for

$\{\ddot{q}^*\}_{t_i}$ into Eq. 16 leads to

$$\{\Delta q^*\}_{t_{i+1}} = [M + D (\Delta t/2)]^{-1} \left([M - D (\Delta t/2)] \{\Delta q^*\}_{t_i} + \{C\}_{t_i} \right) \tag{18}$$

10

which is equivalent to $\{\triangle q*\}_{t_{i+1}}$ given by Eqs. 11 and 13 when D is a null matrix and $\{\dot{q}_I^*\}$ is not considered.

The mass matrix [M] is developed in BR-1 using the lumped mass approach and is given by (Eq. A-97, Ref. 1)

$$[M] = \begin{bmatrix} [M_1] & & & \\ & [M_2] & & O \\ & & \ddots & \\ & & & \ddots \\ & O & & \ddots \\ & & & & [M_R] \end{bmatrix} \tag{19a}$$

where $[M]_r$ is a 6x6 matrix given by

$$[M]_r = \sum_{n_r} [J_n]^T [m_{n_\alpha}] [J_n] \quad \alpha \leftarrow\rightarrow r \tag{19b}$$

and $[m_{n_\alpha}]$ is a diagonal matrix of the lumped mass at the α node of the nth element. Comparing Eq. 10b with Eq. 19a reveals that the two matrices $[M + D (\triangle t/2)]$ and $[M - D (\triangle t/2)]$ occupy the same nonzero 6x6 locations as the original matrix M. Thus, the same procedure used in BR-1 to compute $[M]^{-1}$ can be used to compute $[M + D (\triangle t/2)]^{-1}$. Its only necessary to modify the elements of $[M]_r$ by the addition of the damping matrix $[D]_r$ given by Eq. 10c. The other necessary change is the addition of the Matrix $[M - D (\triangle t/2)]$ as a product with $\{\triangle q*\}_{t_i}$.

Thus since

$$\underline{M}^{-1} = \begin{bmatrix} [M_1]^{-1} & & & \\ & [M_2]^{-1} & 0 & \\ & & \ddots & \\ 0 & & & \ddots \\ & & & & [M_R]^{-1} \end{bmatrix} \qquad (20)$$

Eq. 18 can be expressed in the form

$$\{\triangle q^*\}_{rt_{i+1}} = [M_r + D_r \, (\triangle t/2)]^{-1} \left([M_r - D_r \, (\triangle t/2)] \, \{\triangle q^*\}_{rt_i} \right. \qquad (21)$$

$$\left. + \{C\}_{rt_i} \right) , \qquad\qquad r = 1, 2, \ldots R$$

C. Program Changes and Modification Logic

The following routines of the IBM version of BR-1 have been modified for BR-1HR: MAIN, MEMBER, MTERM, QPLATE, STØRE, DELTT, DEFLX, REVIV1 and REVIV2. Two new subroutines were created: DPMASS and ADDAMP. The core size was increased from 250k bytes to 290k bytes.

The flow of the logic of the modifications is as follows:

1. Compute $[M]_r$ in   STØRE   (no change)

2. Compute $[D]_r$ in   STØRE

3. Compute $[M]_r^{-1}$ in   MTERM   (no change)

4. Compute maximum time interval for numerical stability in DELTT
    based on $[M]$ (no change)

5. Take the inverse of $[M]_r^{-1}$ to get $[M]_r$ in DPMASS using INVS

6. Compute $[M_r + D_r \,(\Delta t/2)]$ and $[M_r - D_r \,(\Delta t/2)]$ in DPMASS

7. Compute $[M_r + D_r \,(\Delta t/2)]^{-1}$ in DPMASS using INVS

8. Compute $[M_r + D_r \,(\Delta t/2)]^{-1} \, [M_r - D_r \,(\Delta t/2)]$ in DPMASS

9. Compute $[M_r + D_r \,(\Delta t/\Delta)]^{-1} \, [M_r - D_r \,(\Delta t/\Delta)] \, \{\Delta q^*\}_{t_i}$ in ADDAMP

10. Compute $\{\Delta q^*\}_{t_{in}}$ using Eq. 21 in DEFLX (no change)

The phrase "no change" means that the original procedure was used. When no damping is considered the modifications and additions are bypassed.

13

III. USER'S INSTRUCTIONS FOR BR-1HR

The instructions for the use of the BR-1 code are given in Ref. 2.
All of the instructions contained in that volume also apply to the modi-
fied program BR-1HR. The time step for numerical stability of BR-1HR
is identical to that of BR-1. The additional instructions required to
use BR-1HR are as follows:

1. Problem Control Card (page 4, Ref. 2)

    IHR (I5, Col. 66-70) - IHR = 0, no fluid is involved; the

    (follows IREV)   original BR-1 code is used. IHR = 1,

           fluid is involved, the modifications

           are used.

2. Rectangular Panel Card (page 8, Ref. 2)

    RHØCF (E8.4, Col. 55-62) - RHØCF is the product of γ_f, the

    (between RHØ and Table   <u>fluid specific weight</u>, and c, the
    CØDE)

           sonic velocity of the fluid. The

           units of $\gamma_f c$ are $lb_f -in.^{-2} - sec.^{-1}$

           If the panel is not in contact

           with the fluid, RHØCF = 0.

IV. SAMPLE PROBLEM

A simply supported square plate is subjected to a step pressure load
of the form

$$p = o \qquad\qquad t = o$$

$$p = P \sin \frac{\pi x}{a} \sin \frac{\pi y}{a} \qquad\qquad t \geq o \qquad\qquad (22)$$

Due to symmetry, only one quarter of the plate is considered: The
parameters of the problem are:

$E = 10.4 \times 10^6$ psi — Young's modulus

$\gamma = 0.0965$ lb/in^3 — specific weight of the plate

$\upsilon = 1/3$ — Poisson's ratio

$h = 0.1$ in. — thickness

$a = 20$ in. — length and width

$P = 0.01$ lb/in^2

The load is sufficiently small such that the nonlinear effects are
negligible. The plate is modeled with four elements as shown in Fig. 1.

The equation governing the damped motion of the plate corresponding
to Eq. 16 is

$$D\nabla^4 w + \frac{\gamma h}{g} \ddot{w} + \rho c \dot{w} = P \sin \frac{\pi x}{a} \sin \frac{\pi y}{a} \qquad\qquad (23)$$

where

$$D = \frac{Eh^3}{12(1-\upsilon^2)} \; , \qquad \nabla^4 = \frac{\partial^4}{\partial x^4} + 2 \frac{\partial^4}{\partial x^2 \partial y^2} + \frac{\partial^4}{\partial y^4}$$

and g is the local acceleration due to gravity. The solution to Eq.
23 is
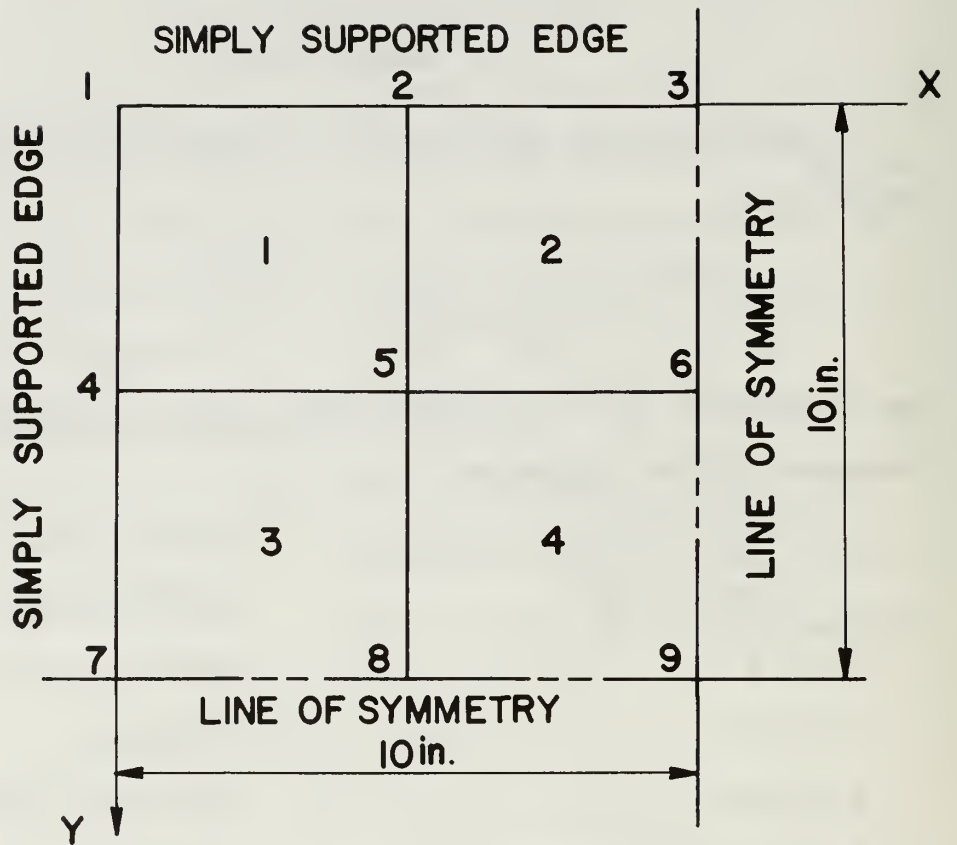
FIGURE I.   SAMPLE PROBLEM

$$w = w_{st} \{1 - e^{-\zeta\omega t} \cos (\sqrt{1 - \zeta^2}\,\omega t + \varphi) / \cos \varphi\} \qquad (24)$$

where

$$\tan \varphi = - \zeta / \sqrt{1 - \zeta^2}$$

$$w_{st} = \frac{a^4 P}{4D\pi^4} \sin \frac{\pi x}{a} \sin \frac{\pi y}{a}$$

$$\zeta = \frac{\rho cg}{2\gamma h}$$

$$\omega = \frac{2\pi^2}{a^2} \sqrt{\frac{Dg}{h\gamma}}$$

when the plate is initially at rest. The displacement at the center of the plate given by Eq. 24 is plotted in Figures 2, 3, and 4 as a function of time for ζ = 0, 0.666 and 270 corresponding to zero damping, less than critical damping and very heavy damping respectively. The corresponding values of $g\rho c$ for the fluid are 0, 4, and 1620 lb_f /(in^2-sec). Also plotted in Figs. 2-4 are the results from BR-1HR. The input data sheets and the print of the input data are given in Fig. 5. The execution time on the IBM 360/67, FORTRAN IV - Level H, was 8 min. and 26 sec. for 200 time steps with ζ = 270. The run with damping not considered took essentially the same length of time.

17
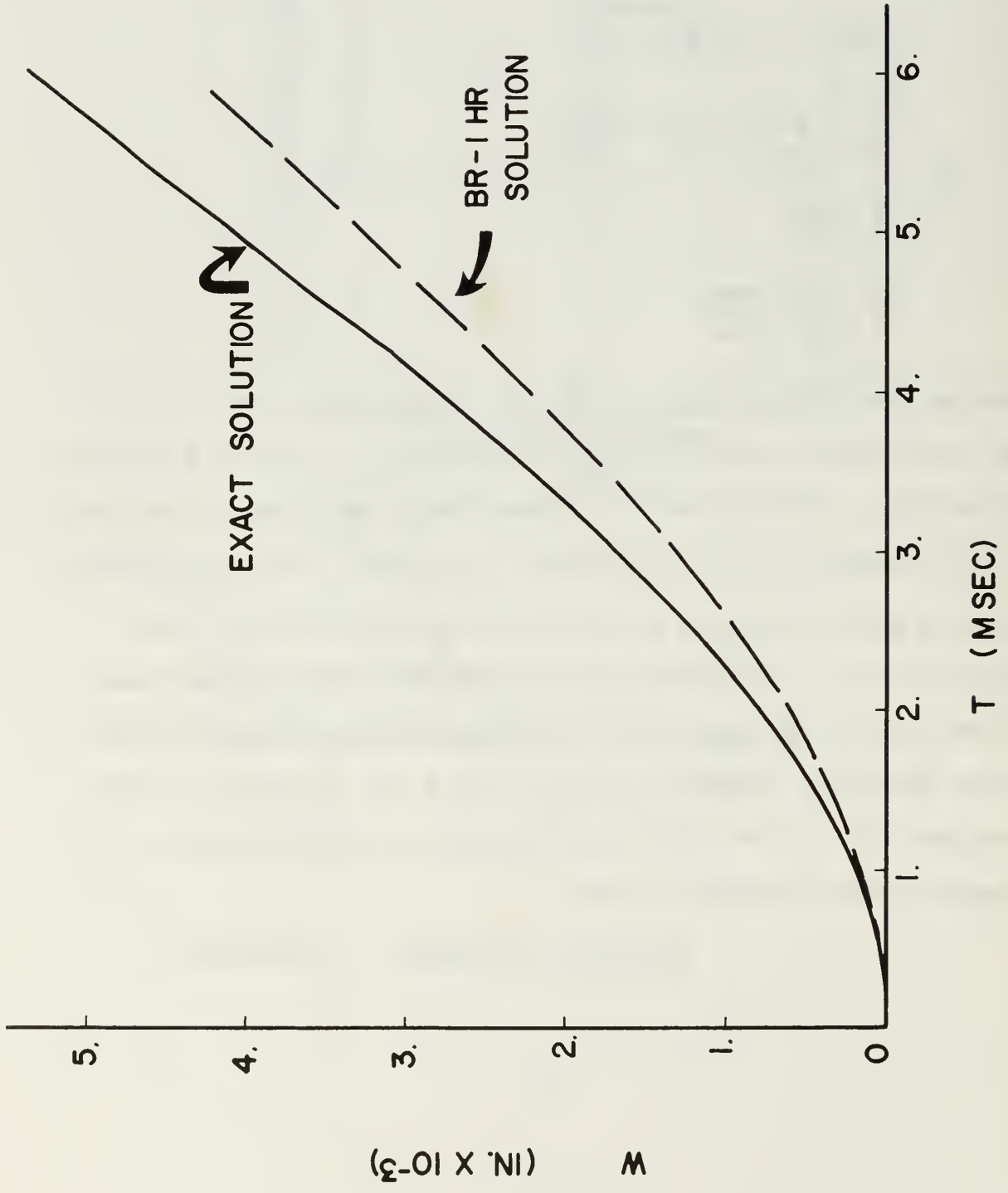
FIGURE 2. TRANSVERSE DISPLACEMENT AT NODE 9 VERSUS TIME, $f = 0$ (NO DAMPING)
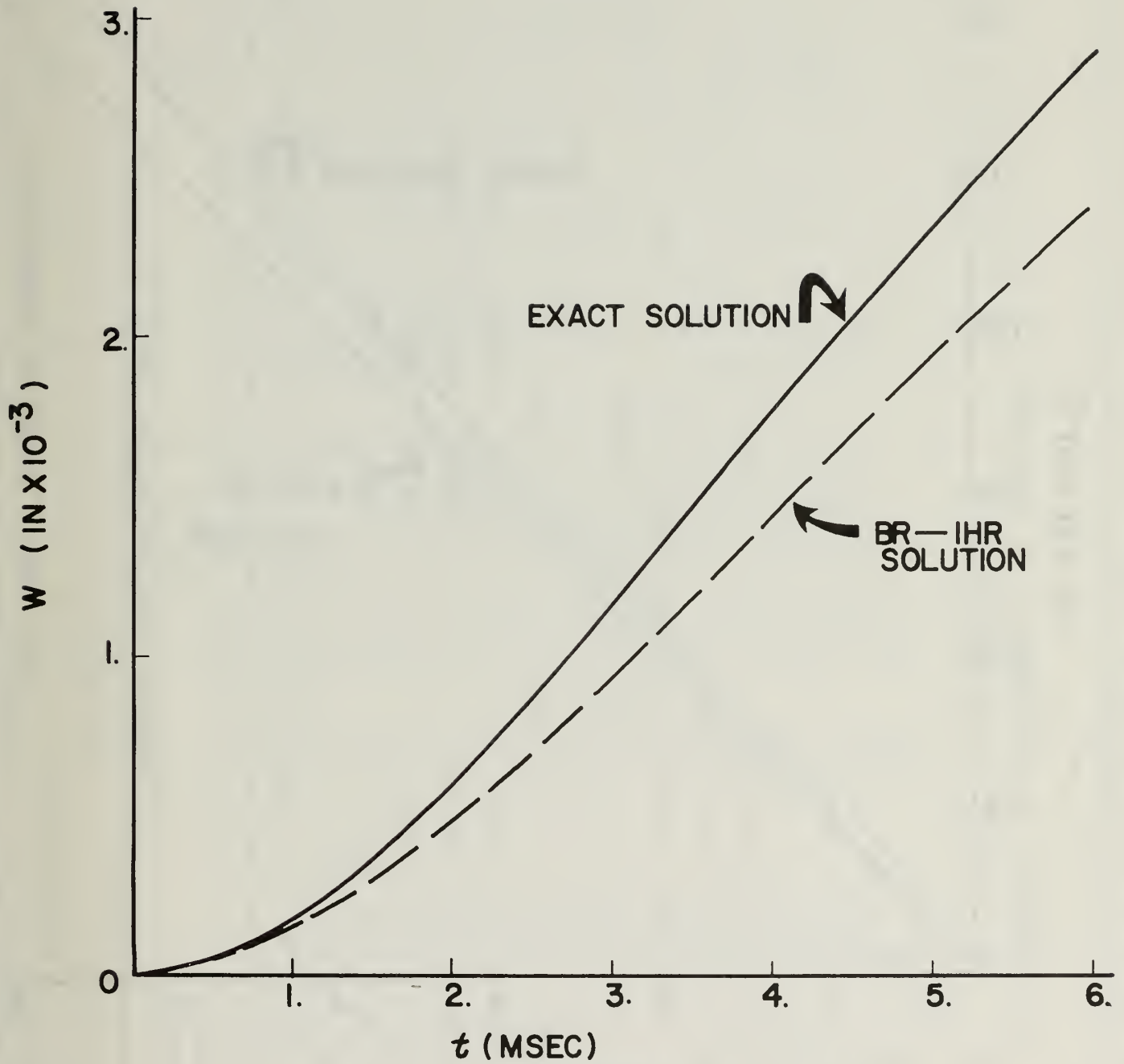
FIGURE 3.   TRANSVERSE   DISPLACEMENT AT NODE 9 VERSUS
TIME, f = 0.666

19
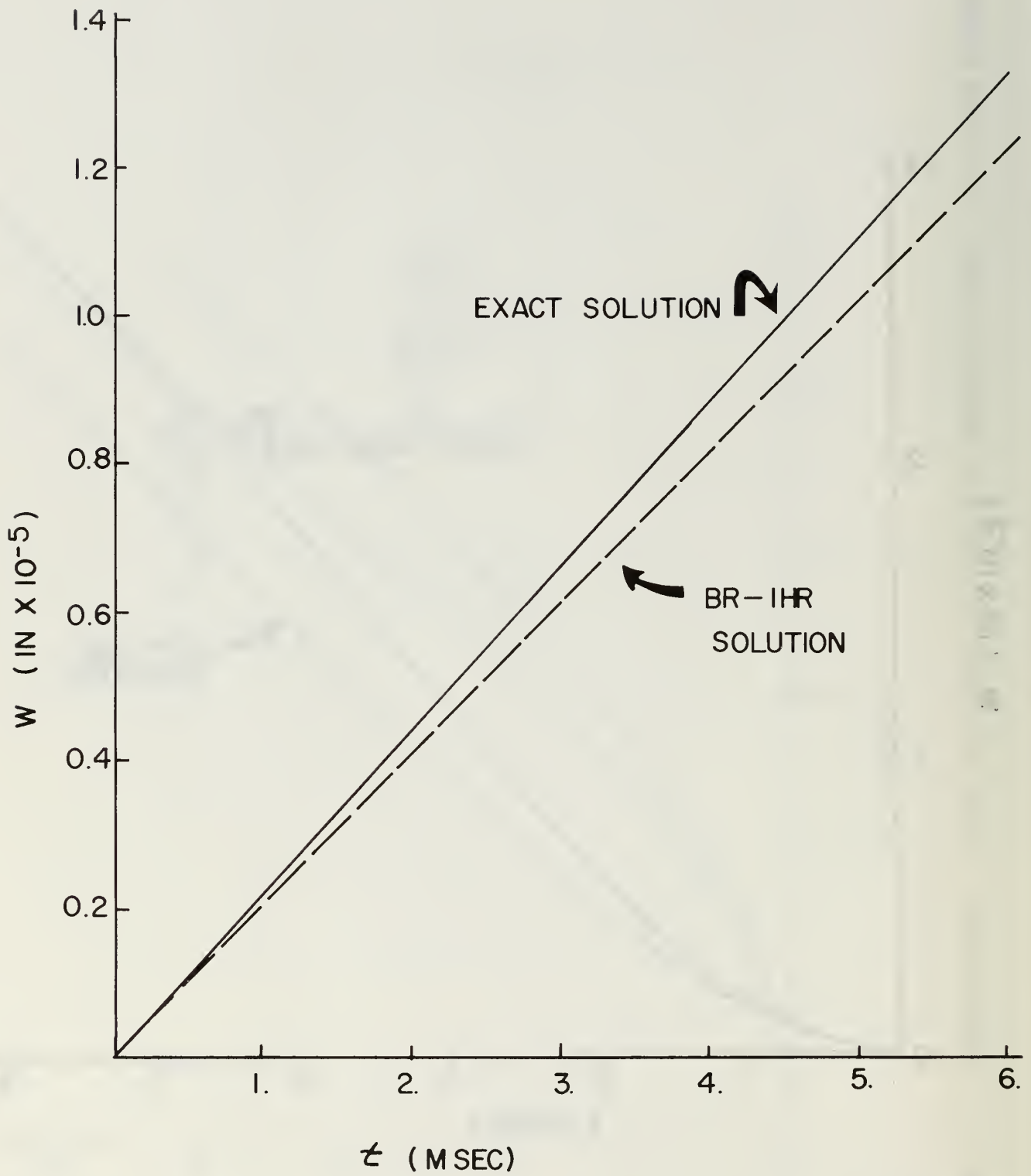
FIGURE 4. TRANSVERSE DISPLACEMENT AT NODE 9 VERSUS
TIME, $f = 270$

PROGRAMMER R.E. BALL

PROGRAM: BR-1HR, SAMPLE PROBLEM

PAGE 1 OF 1

SPECIAL INSTRUCTIONS

CARD PUNCH OPERATOR

DATE COMPLETED

GENERAL PURPOSE CODING FORM

0 = ZERO   Ø = ALPHA O   1 = ONE   I = ALPHA I   2 = TWO   Z = ALPHA Z

A TEST CASE FOR THE M-R VERSION OF BR-1, (BR-1HR) WITH DAMPING, RHØ*C=1620

9		4	37	50	1	0	80	0	2	5	0 1
1		5	2	4	10.4	.1	.3333	.0965	1620.		1.
2		6	3	5	10.4	.1	.3333	.0965	1620.		1.
4		8	5	7	10.4	.1	.3333	.0965	1620.		1.
5		9	6	8	10.4	.1	.3333	.0965	1620.		1.
1		0.	0.	0.	0.	2.	5.	0.
3		10.	0.	0.	4.	0.	5.	0.
5		5.	5.	0.	6.	10.	5.	0.
7		0.	10.	0.	8.	5.	10.	0.
9		10.	10.	0.
1		1 1	2 1	3 1	4 1	6 2	1 2	2 2	3 2	5 2	6
3		1 3	2 3	3 3	5 3	6 4	1 4	2 4	3 4	4
6		1 6	5 6	6 7	1 7	2 7	3 7	4 7	6
8		6 9	1 9	2 9	4 9	5 9	6 8	2 8	7
1		0	3	0	0	0	.95
0.				0	0	4	10.4E+6	1.
1.	.001464	2	.003535	3	.003535	4	.008535

CODING SHEET 12ND NPS 5220/1 (Rev. 3/74) ☆ GPO 708-888

EIGHTY COLUMN

Figure 5. Input Data Sheet

21

V. SUMMARY AND CONCLUSIONS

The finite element digital computer code BR-1 developed by the Northrop
Corporation for predicting the effects of internal air blast on typical
combat aircraft skin-rib-stringer structures has been modified to include
the effect of compressible fluid-structure interaction. The fluid-structure
interaction is approximated by the piston theory wherein the effect of the
fluid upon the structure is accounted for by introducing damping to the
equations of motion of the structure. The modified code is called BR-1HR.
This code, in conjunction with the NWC code for predicting hydraulic ram
pressures, can be used to predict the structural response of aircraft fuel
tanks subjected to penetrating bullets and fragments.

All of the features of BR-1 exist in BR-1HR, and only two additional
numbers are required for the input data. The modified code is operational
on the IBM 360/67 in FORTRAN IV, level H, and requires 290K bytes of
storage. A sample problem was executed to demonstrate the validity of the
modified code for zero damping, less than critical damping, and very heavy
damping.

VI. REFERENCES

1. Brass, J., Yamane, J. R., and Jacobson, M. J., "Effects of Internal Blast on Combat Aircraft Structure, Volume I. Engineer's Manual," Air Force Flight Dynamics Laboratory, Tech. Rpt. AFFDL-TR-73-136, Vol. I, Jan. 1974.

2. Brass, J., Yamane, J. R., and Jacobson, M. J., "Effects of Internal Blast on Combat Aircraft Structure, Volume II. User's and Programmer's Manual," Air Force Flight Dynamics Laboratory Tech. Rpt. AFFDL-TR-73-136, Vol. II, Jan. 1974.

3. Lundstrom, E., "Fluid Dynamic Analysis of Hydraulic Ram," Naval Weapons Center, NWC TP 5227, July 1971.

4. Bedrosian, B. and DiMaggio, F. L., "Acoustic Approximations in Fluid-Shell Interactions," J. Eng. Mech. Div., ASCE, Vol. 98, No. EM3, pp 731-742, June 1972.

5. Klosner, J. M., "Inadequacies of Piston Theory in Fluid-Shell Interactions," J. Eng. Mech. Div., ASCE, Vol. 96, No. EM2, pp 143-159, April, 1970.

6. Fuhs, A. E., Ball, R. E., and Power, H. L., "FY 73 Hydraulic Ram Studies," Naval Postgraduate School, NPS-57Fu74021, Feb. 1974.

7. Lundstrom, E., "Method of Hydraulic Ram Fluid Structures Analysis-
    An Outline," Naval Weapons Center Working Paper, China Lake, CA.

APPENDIX - A STUDY OF THE ACCURACY AND STABILITY OF SEVERAL NUMERICAL
INTEGRATION SCHEMES FOR THE TRANSIENT RESPONSE OF HEAVILY DAMPED
STRUCTURES

Many studies have been made of the accuracy and stability of
numerical integration schemes for the equations of motion of structural
systems. However, most of these studies concentrate on the response of
undamped, or lightly damped, systems. Of interest here is the response
of both lightly damped and heavily damped systems since both kinds of
damping can occur when a structure is vibrating in contact with a
compressible fluid (6).

The equations of motion of the system under consideration are given
in matrix form by Eq. 16. Three different finite difference schemes for
the numerical solution of these equations are considered here. Only
explicit, non-iterative schemes are considered due to the fact that the
BR-1 code uses an explicit solution procedure. Two of the three schemes
are based upon a two variable approach using $\{q^*\}$ and $\{v^*\}$, where

$$\{\dot{q}^*\} = \{v^*\} \tag{B-1}$$

Thus, Eq. 16 can be given in the form

$$\{\dot{v}^*\} = [M]^{-1} (\{C\} - [D] \{v^*\}) \tag{B-2}$$

First Scheme

Substituting the first order approximations for $\{\dot{v}^*\}$ and $\{\dot{q}^*\}$

$$\{\dot{v}^*\}_{t_i} = (\{v^*\}_{t_{i+1}} - \{v^*\}_{t_i}) / (\Delta t) \tag{B-3a}$$

$$\{\dot{q}^*\}_{t_{i+1}} = (\{q^*\}_{t_{i+1}} - \{q^*\}_{t_i})/(\Delta t) = \{\Delta q^*\}_{t_i} /(\Delta t) \qquad \text{(B-3b)}$$

into Eqs. B-1 and B-2 leads to

$$\{v^*\}_{t_{i+1}} = [I - M^{-1}D\,(\Delta t)]\,\{v^*\}_{t_i} + (\Delta t)\,[M]^{-1}\,\{C\}_{t_i} \qquad \text{(B-4a)}$$

$$\{\Delta q\}_{t_{i+1}} = \Delta t\,\{v^*\}_{t_{i+1}} \qquad \text{(B-4b)}$$

Eliminating $\{v^*\}$ from Eqs. B-4 results in

$$\{\Delta q^*\}_{t_{i+1}} = [I - M^{-1}D\,(\Delta t)]\,\{\Delta q^*\}_{t_i} + (\Delta t)^2\,[M]^{-1}\,\{C\} \qquad \text{(B-5)}$$

This is identical to the scheme used in BR-1 when damping is not considered. It is also equivalent to the scheme where the acceleration $\{\ddot{q}^*\}$ is approximated by the conventional central difference approximation, Eq. 17a. The two variable approach given by Eqs. B-4 may be more desirable than Eq. B-5 due to roundoff error considerations, i.e. $(\Delta t)^2$ in Eq. B-5 is a very small number.

Second Scheme

The second scheme uses Eq. B-4a and the simple forward Euler approximation for $\{v^*\}$ in Eq. B-1

$$\{\Delta q^*\}_{t_{i+1}} = (\Delta t)\,\{v^*\}_{t_i} \qquad \text{(B-6)}$$

in place of the backward approximation of Eq. B-4b. The solution procedure is to compute $\{v^*\}_{t_{i+1}}$ using Eq. B-4a and $\{\Delta q^*\}_{t_{i+1}}$ using Eq. B-6.

Third Scheme

The third scheme uses the conventional central difference approxi-

mations for both $\{\dot{q}*\}$ and $\{\ddot{q}*\}$, i.e. Eqs. 15 and 17a. This gives Eq. 18, reproduced here for convenience

$$\{\Delta q*\}_{t_{i+1}} = [M + D\ (\Delta t/2)]^{-1}\ ([M - D\ (\Delta t/2)]\ \{\Delta q*\}_{t_i} + (\Delta t)^2\ \{C\}_{t_i})\quad (B-7)$$

This scheme is also identical to the BR-1 scheme when damping is not considered. A two variable version of this scheme is

$$\{\Delta v*\}_{t_{i+1}} = [M + D\ (\Delta t/2)]\ ([M - D\ (\Delta t/2)]\ \{\Delta v*\}_{t_i} + (\Delta t)\ \{C\}_{t_i})\quad (B-8a)$$

and

$$\{\Delta q*\}_{t_{i+1}} = (\Delta t)\ \{\Delta v*\}_{t_{i+1}}\quad (B-8b)$$

This may have smaller roundoff error than Eq. B-7 since $(\Delta t)^2$ has been eliminated.

The Single Degree of Freedom, Damped Oscillator

The equation for the free vibrations of the single degree of freedom, damped oscillator is

$$m\ddot{q} + d\dot{q} + hq = 0\quad (B-9)$$

Applying the three schemes described above to Eq. B-9 leads to

$$q_{t_{i+1}} - (2 - 2\ \zeta\bar{\omega} - \bar{\omega}^2)\ q_{t_i} + (1 - 2\zeta\bar{\omega})q_{t_{i-1}} = 0\quad (B-10a)$$

$$\begin{bmatrix} 1 & 0 \\ 0 & 1 \end{bmatrix} \left\{ \begin{matrix} (\Delta t)v \\ q \end{matrix} \right\}_{t_{i+1}} - \begin{bmatrix} 1 - 2\zeta\bar{\omega} & -\bar{\omega}^2 \\ 1 & 1 \end{bmatrix} \left\{ \begin{matrix} (\Delta t)v \\ q \end{matrix} \right\}_{t_i} = 0\quad (B-10b)$$

$$(1 + \zeta\bar{\omega})q_{t_{i+1}} - (2 - \bar{\omega}^2)q_{t_i} + (1 - \zeta\bar{\omega})q_{t_{i-1}} = 0\quad (B-10c)$$

27

where

$$\bar{\omega} = (\Delta t)_\omega \qquad \omega = \sqrt{h/m} \qquad \zeta = d/(2m_\omega)$$

according to Eqs. B-5, B-4a and B-6, and B-7, respectively.

The solution to Eq. B-9 can be given in the form

$$q_{t_i} = A \left(e^{-\zeta\bar{\omega}} \, e^{\mp\bar{\omega}\sqrt{\zeta^2-1}} \right)^i = (A\lambda_c)^i \qquad \text{(B-11)}$$

where A is an arbitrary constant and the superscript i denotes the ith power. The solution to the three difference schemes for an arbitrary set of initial conditions can be obtained by assuming

$$q_{t_i} = A\lambda^i \qquad \text{(B-12a)}$$

$$(\Delta t)v_{t_i} = B\lambda^i \qquad \text{(B-12b)}$$

where λ, A and B are unknown constants. Substituting Eqs. B-12 into Eqs. B-10 and solving for λ for each scheme lead to

$$\lambda_1 = 1 - \zeta\bar{\omega} - \bar{\omega}^2/2 \mp \bar{\omega}\sqrt{(\zeta + \bar{\omega}/2)^2 - 1} \qquad \text{(B-13a)}$$

$$\lambda_2 = 1 - \zeta\bar{\omega} \mp \bar{\omega}\sqrt{\zeta^2 - 1} \qquad \text{(B-13b)}$$

$$\lambda_3 = (1 - \bar{\omega}^2/2 \mp \bar{\omega}\sqrt{\zeta^2 + \bar{\omega}^2/4 - 1} \;) /(1 + \zeta\bar{\omega}) \qquad \text{(B-13c)}$$

When the discriminant in Eqs. B-11 and B-13 is positive the solution consists of damped motion only. When it is negative the motion is damped and oscillatory. Thus, a zero discriminant defines the limit of the oscillatory behavior.

The accuracy of the three numerical schemes can be evaluated by comparing λ_1, λ_2 and λ_3 with λ_c for several values of ζ and $\bar{\omega}$. The values of the ratios of the numerical solution to λ_c are given in Table B-1 for $\zeta = 0$, 0.5, 5, and 500 and $\bar{\omega} = 0.1$. This value of $\bar{\omega}$ corresponds to a time step of 1 μ sec when $\omega = 100,000$ rad/sec or a time step of 1 msec when $\omega = 100$ rad/sec, etc., i.e. the solution is computed ten times over the time interval $1/\omega$ or 20π times over the undamped natural period $2\pi/\omega$. The closer the ratio in Table B-1 is to one, the closer the numerical eigenvalue is to the correct eigenvalue.

The numerical stability of each scheme can also be determined from Eqs. B-13. When $|\lambda| > 1$ the numerical solution will be unstable. The upper limit on $\bar{\omega}$ for stability can be determined for a given value of ζ by equating $|\lambda|$ to one and solving for $\bar{\omega}$. When the discriminant is positive $\lambda = -1$ is the limiting value and the negative sign in the $\mp$ applies. When the discriminant is negative $|\lambda| = \sqrt{x^2 + y^2}$ where x and y are the real and imaginary parts respectfully. The results for the limiting values of $\bar{\omega}$ for an oscillatory solution and for numerical stability are given in Table B-2.

Scheme	$\zeta = 0$	$\zeta = 0.5$	$\zeta = 5$	$\zeta = 500$
λ_1/λ_c	$0.999999 \mp i$ 0.000042	$0.997322 \mp i$ 0.001542	$1.00005,$ 0.000002	$1.00001,$ -0.9218×10^{10}
λ_2/λ_c	$1.00499 \mp i$ 0.000333	$1.00284 \mp i$ 0.004319	$0.999949,$ 0.027185	$1.00000,$ -0.9213×10^{10}
λ_3/λ_c	$0.999999 \mp i$ 0.000042	$0.999959 \mp i$ 0.000072	$1.00000,$ 0.906095	$1.00000,$ -0.3969×10^{9}
λ_c	$0.995004 \mp i$ 0.099833	$0.947665 \mp i$ 0.082275	$0.989949,$ 0.371615	$0.999495,$ 0.2062×10^{-8}

TABLE B-1. Comparison of Numerical and Exact Solutions

30

Scheme	Oscillatory limit	Stability limit
λ_1	$\bar{\omega} = 2(1-\zeta)$	$\bar{\omega} = 2(\sqrt{\zeta^2 + 1} - \zeta)$
λ_2	$\zeta = 1$	$\bar{\omega} = 2\zeta, \ \zeta \leq 1$ $\bar{\omega} = 2\zeta - 2\sqrt{\zeta^2 - 1}, \ \zeta \geq 1$
λ_3	$\bar{\omega} = 2\sqrt{1 - \zeta^2}$	$\bar{\omega} = 2$

TABLE B-2   Limits on $\bar{\omega}$ for an Oscillatory Solution and a Stable Solution

Note that λ_2 is unstable for any non-zero value of $\bar{\omega}$ when $\zeta=0$ and that 2 is the maximum limit on $\bar{\omega}$ for all three schemes. Also note that the limit on λ_3 is the same as that on the BR-1 routine, even with damping, and that this is the least restrictive scheme. Consequently, based upon these accuracy and stability considerations the third scheme is selected.

DISTRIBUTION LIST

<div align="right">No. of Copies</div>

1. Library   2
   Code 0212
   Naval Postgraduate School
   Monterey, CA   93940

2. Defense Documentation Center   2
   Cameron Station
   Alexandria, VA   22314

3. Department of Aeronautics
   Code 57
   Naval Postgraduate School
           Prof. R. W. Bell   1
           Assoc. Prof. R. E. Ball   10
           Asst. Prof. H. Power   1

4. Dean of Research   1
   Code 023
   Naval Postgraduate School
   Monterey, CA   93940

5. Naval Weapons Center
   China Lake, CA   93955
           Attn: Mr. Wallace Fung   2
                   Code 5114

6. Dr. M. L. Jacobson   1
   Orgn 3761/62
   Northrop Corporation
   3901 W. Broadway
   Hawthorne, CA   90250

7. AFFDL (CC)   1
   Wright-Patterson AFB, OH   45433

8. AFFDL (PT)
   Wright-Patterson AFB, OH   45433   1

9. AFFDL (PTS)   10
   Wright-Patterson AFB, OH   45433

10. AFFDL (TST)   1
    STINFO
    Wright-Patterson AFB, OH   45433

11. ASD (YHEX)   1
     Attn: J. Rievley
     Wright-Patterson AFB, OH   45433

12. AFIT (ENB)   1
     Attn: Dr. Torvik
     Wright-Patterson AFB, OH   45433

13. US Army Ballistic Research Labs   1
     Code AMXBR VL
     Attn: Candless
     Aberdeen Proving Ground, MD   21005

14. US Army Air Mobility R and D Labs   1
     Attn: Pedriani
     Eustis Directorate Savol Eu Mos
     Fort Eustis, VA   23604

15. The Boeing Co Vertol Division   1
     Boeing Center
     Attn: Gonsalves
     P. O. Box 16858
     Philadelphia, PA   19142

16. Bell Helicopter Co.   1
     Textron, Inc. Division
     Attn: Morris
     P. O. Box 482
     Fort Worth, TX   76101

17. The Boeing Company   1
     Wichita Division
     3801 South Oliver St.
     Wichita, KS   67210

18. The Boeing Company   1
     Aerospace Group
     Attn: Bristow
     P. O. Box 3999
     Seattle, WA   98124

19. Fairchild Industries, Inc.   1
     Fairchild Republic Division
     Farmingdale, NY   11735

20. Dynamic Science Division   1
     Ultrasystems, Inc.
     Attn: Zabel
     1850 W. Pinnacle Peak Rd.
     Phoenix, AZ   85027

21. The Firestone Tire & Rubber Co.   1
     Firestone Coated Fabrics Div.
     P. O. Box 869
     Magnolia, AR 71753

22. General Dynamics Corporation   1
     Convair Aerospace Division
     P. O. Box 748
     Fort Worth, TX 76101

23. Goodyear Tire & Rubber Company   1
     Aviation Products Division
     1144 E. Market St.
     Akron, OH 44136

24. Grumman Aerospace Corporation   1
     Attn: Henze
     South Oyster Bay Road
     Bethpage, LI, NY 11714

25. Hughes Tool Company   1
     Aircraft Division
     Centinela & Teale St.
     Culver City, CA 90230

26. Lockheed Aircraft Corporation   1
     Attn: Cook
     2555 N. Hollywood Ave.
     Burbank, CA 90808

27. McDonnell Douglas Corporation   1
     Douglas Aircraft Co.
     Attn: W. S. Lowe
     3855 Lakewood Blvd.
     Long Beach, CA 90801

28. Northrop Corporation
     Aircraft Division-Tech Library
     3901 West Broadway
     Hawthorne, CA 90250
     Attn: Bach   1
            Yamane   1
            Jacobson   1

29. LTV Aerospace Corporation   1
     Vought Systems Division
     Attn: Dan Reedy
     P. O. Box 5907
     Dallas, TX 75222

30. McDonnell Douglas Corporation McDonnell Aircraft Company Attn: Wiggens P. O. Box 516 St. Louis, MO 63166	1
31. Rockwell International Columbus Aircraft Division Attn: Morrow 4300 East Fifth Avenue Columbus, OH 43216	1
32. R & D Associates Attn: H. L. Brode 525 Wilshire Blvd. P. O. Box 3580 Santa Monica, CA 90403	1
33. Rockwell International B-1 Division International Airport Los Angeles, CA 90009 Attn: Dotseth S. Mellin	 1 1
34. Uniroyal, Inc. Attn: Galloway 312 North Hill St. Mishawaka, IN 46544	1
35. Naval Weapons Center Attn: Code 5114 (D.B. Atkinson) China Lake, CA 939555 Lundstrom	2 1

U165405